
Article:
Luo, P., Long, H.Y., Sweet, M.R. et al. (2 more authors) (2018) Numerical Analysis of 3-Dimensional Scaling Rules on a 1.2-kV Trench Clustered IGBT. IEEE Transactions on Electron Devices, 65 (4). pp. 1440-1446. ISSN 0018-9383

https://doi.org/10.1109/TED.2018.2807318

Numerical Analysis of 3-Dimensional Scaling Rules on a 1.2-kV Trench Clustered IGBT

Peng Luo, Hong Yao Long, Mark R. Sweet, Merlyne De Souza and E. M. S. Narayanan, *Senior Member, IEEE*

***Abstract*— 3-dimensional scaling rules for the cathode cells and threshold voltages of a 1.2-kV Trench Clustered IGBT (TCIGBT) are investigated using calibrated models in Synopsys Sentaurus TCAD tools. Scaling down results in an enhancement of current gain of the inherent thyristor action which reduces the forward voltage drop even more than that of a scaled Trench IGBT (TIGBT). For identical switching losses, at a scaling factor k=3, the forward voltage drop is reduced by 20% at 300K and 30% at 400K when compared to the conventional TCIGBT (k=1). Most importantly, despite its lower conduction losses than an equivalent TIGBT, a scaled TCIGBT structure can maintain its short circuit capability, due to the additional scaling principle applied to the n-well and p-well regions, maintaining the self-clamping feature. Thus, TCIGBT is a more efficient chip-for-chip, reliable replacement of a TIGBT for energy savings in applications.**

***Index Terms*—IGBT, Clustered IGBT, $V_{ce(sat)}$ -E_{off} trade-off, power semiconductor device, scaling rule, short circuit capability, self-clamping feature.**

I. Introduction

THE ever increasing demand for energy efficiency in power electronics necessitates reduction in the on-state and switching losses in power semiconductor devices because the increase of power converter efficiency enabled by reduction in device losses can result in 25-40% savings of worldwide electrical energy consumption per annum [1]. From a performance over cost as well as reliability perspective, silicon based power devices will continue to play a crucial role in current and future power electronics systems. Trench gated Insulated Gate Bipolar Transistors (TIGBT) are the main power switching devices used today for voltages up to 1.7 kV. They are widely used in high power converters, Pulse Width Modulated (PWM) servo and three-phase industry drives requiring high dynamic range control and low harmonics. Significant efforts have been made to reduce their on-state and switching power losses because of their direct impact on energy savings. Most recently, a "More-than-Moore" concept [2] has been extended to IGBTs to enhance their power densities and ensure compatibility with nanometric CMOS technology. The scaling concept proposed for the Trench gated IGBT [3, 4] showed significant lowering of the on-state voltages ($V_{ce(sat)}$) due to the Injection Enhancement (IE) effect [5]. The IE effect can be defined as a mechanism to enhance electron concentration within the drift region of an IGBT beyond that realized purely by MOS channel conduction. This effect increases the drift region cathode side carrier concentration and enables a p-i-n diode like carrier profile. The same effect is used in 1D scaling of mesa width [6], 2D and 3D scaling of cathode cells [3, 4] as well as deep sub-micron designs [7]. However, the IE effect also results in non-saturation of the MOS channel current, leading to significant degradation of short circuit withstand capability [8, 9]. During the short-circuit mode, devices need to sustain simultaneously high voltage and high current, causing a significant increase in the local device temperature due to high-power dissipation. The device must survive under such abnormal conditions until the system protection circuit shuts down the driving signal. The reduction in short circuit capability in scaled TIGBT is attributed to the Collector Induced Barrier Lowering (CIBL) effect [8], which is caused by conductivity modulation in the MOS channels [9].

Unlike the IE effect in TIGBTs, The Trench Clustered IGBT (TCIGBT) utilizes controlled thyristor action (pnpn effect) to reduce on-state losses [10]. Moreover, TCIGBT exhibits a unique self-clamping feature to protect the cathode cells and achieve low saturation currents without sacrificing on-state forward voltage drop.

In this paper, 3-dimentional scaling rules for the 1.2-kV Field-Stop TCIGBT are investigated in depth, using models which are calibrated against experimental data in [4]. Despite introduction of the n-well and p-well scaling factor (*k/2*), the physics of how self-clamping voltage is scaled while retaining short circuit robustness and blocking voltage is revealed.

II. TCIGBT Physics and Scaling Principle

Fig. 1 presents the top view of the TCIGBT topology design. The unique designed ladder structure features several stripe shaped trenches running in parallel across the active cluster cells. A cross sectional 3-dimensional TCIGBT unit cell as highlighted in Fig. 1 is shown in Fig. 2(a). The thyristor structure consists of n-well, p-well, n-drift and p-anode. To turn

Manuscript received ; revised ; accepted . Date of current version . Recommended for publication by Associate Editor

The authors are with the Electrical Machines and Drives Research Group, Department of Electronic and Electrical Engineering, The University of Sheffield, S1 3JD, U.K. (email: pluo2@sheffield.ac.uk; h.y.long @sheffield.ac.uk; m.r.sweet@sheffield.ac.uk; s.madathil@sheffield.ac.uk).

Colour versions of one or more of the figures in this paper are available on line at http://ieeexplore.ieee.org.

Digital Object Identifier

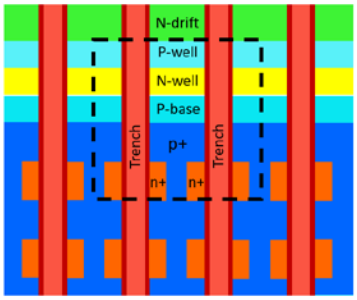

Fig. 1. Top view of the TCIGBT ladder design at the edge of the cluster cell. The highlighted region is the top view of the structure shown in Fig. 2 (a).

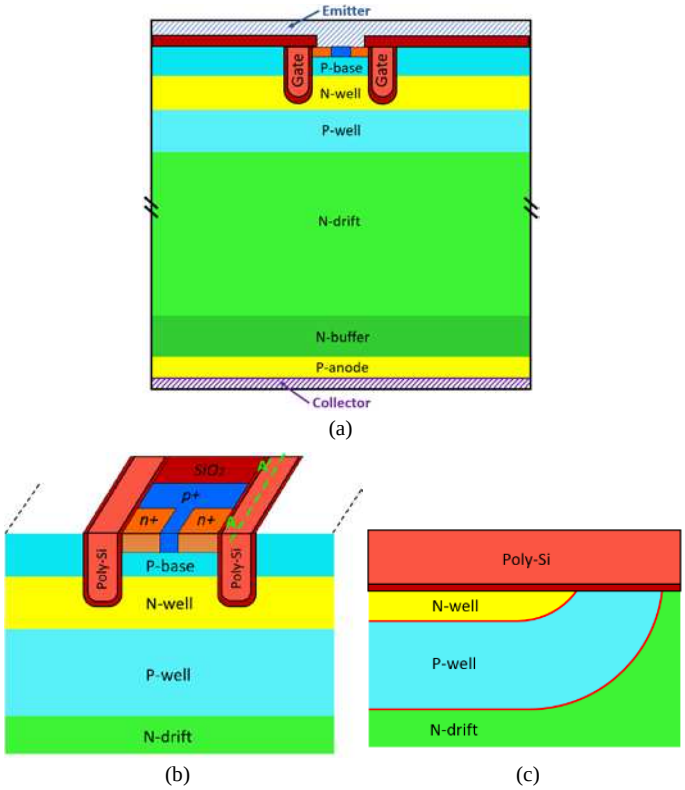

Fig. 2. (a) Schematic cross-section of TCIGBT structure. (b) Cathode structure. (c) Cross-section of cut-line A-A'.

the device ON, a positive gate voltage above the threshold voltage is applied to form inversion layers in both p-well and p-base regions. The inversion layers formed along the walls of the trenches connect the n-well to the ground potential. In addition, as shown in Fig. 2(c), the inversion layers formed below the trench gates connect the n-well with the n-drift and lead to the floating of the p-well region. Therefore, during conduction, the potential in the p-well increases with anode voltage. Once the potential drop across the p-well/n-well junction is sufficient to forward bias the junction barrier, the main thyristor turns on without snap-back in the I-V characteristics. High-level injection of minority carriers results in the removal of the potential barrier across the p-well junction. The conductivity modulation is significantly enhanced because of thyristor action. Hence, the on-state loss is effectively reduced compared to the IGBT structure [10-12].

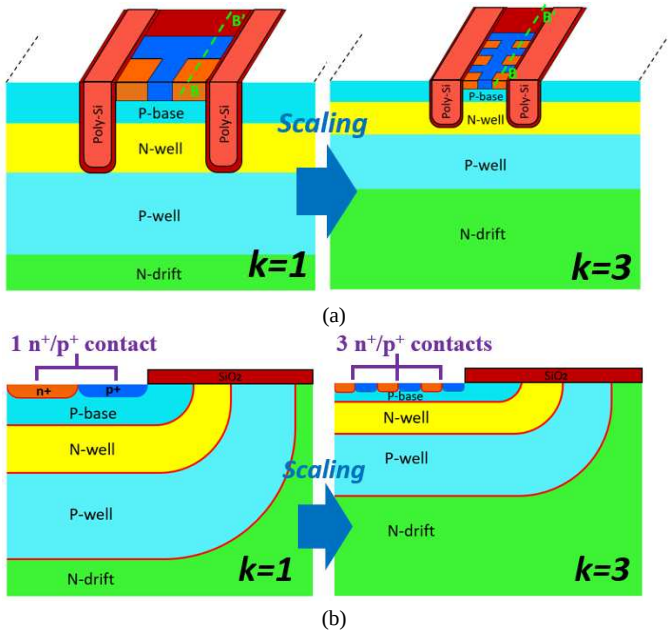

Fig. 3. (a) Scaling principle on 3D TCIGBT structure. (b) Cross-sectional view of cut-line B-B'.

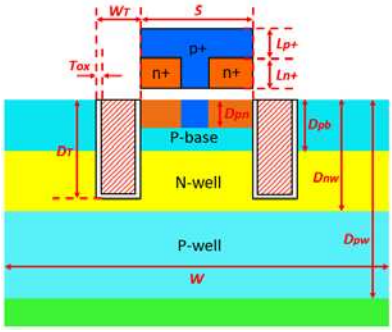

Fig. 4. Parameters specified in TABLE I.

After the TCIGBT structure turns on, current is continuously controlled by the MOS gate. As the p-base/n-well junction is reverse biased, with increase in the anode voltage, the depletion boundary within the n-well region moves towards the p-well junction. Finally, the n-well region will punch through at a pre-defined voltage, termed as "self-clamping" voltage [13]. Any further increase of the anode voltage is supported by the p-well/n-drift junction. Under this condition, the cathode cells are protected from exposure to high anode voltages. More importantly, since the MOS cells are clamped, the saturation current is largely independent of collector voltage and therefore wider Safe Operating Area (SOA) can be achieved. This feature is one of the attractive advantages of CIGBTs.

Fig. 3 shows the concept of 3-dimensional scaling rule on the TCIGBT. More details regarding the structural parameters and scaling rule are shown in Fig. 4 and TABLE I. The cell width *W* is kept identical in all cases for comparison. However, the structural parameters of cluster cells are shrunk as a factor of *k*. The n+/p+ lengths which are perpendicular to the cross-section are shrunk as factor *k* as well to avoid latch-up. Hence, the scaling rule is applied in all the three dimensions. Moreover, it

TABLE I
PARAMETERS AND CHARACTERISTICS APPLIED FOR SCALING RULES.

Parameters & Characteristics	*Symbol/Unit*	*k=1*	*k=2*	*k=3*	*k=4*	*k=5*	*Scaling factor*
Cell Width	$W\ (\mu m)$	10	10	10	10	10	*1*
Trench Width	$W_T\ (\mu m)$	1	1	1	1	1	*1*
Trench Depth	$D_T\ (\mu m)$	4.5	2.25	1.5	1.12	0.9	*k*
Mesa Width	$S\ (\mu m)$	3	1.5	1	0.75	0.6	*k*
n+/p+ Depth	$D_{pn}\ (\mu m)$	0.5	0.25	0.17	0.12	0.1	*k*
n+ Length	$L_{n+}\ (\mu m)$	1.5	0.75	0.5	0.37	0.3	*k*
p+ Length	$L_{p+}\ (\mu m)$	4.5	2.25	1.5	1.12	0.9	*k*
Gate Oxide Thickness	$T_{ox}\ (\mu m)$	0.1	0.05	0.03	0.025	0.02	*k*
P-base Depth	$D_{pb}\ (\mu m)$	2	1	0.67	0.5	0.4	*k*
N-well Depth	$D_{nw}\ (\mu m)$	4.5	4.5	3	2.25	1.8	*k/2*
P-well Depth	$D_{pw}\ (\mu m)$	15	15	10	7.5	6	*k/2*
P-base Doping	cm^{-3}	2×10^{17}	2.4×10^{17}	2.8×10^{17}	3.2×10^{17}	3.6×10^{17}	-
Gate Voltage	$V_g\ (V)$	15	7.5	5	3.75	3	*k*
Threshold Voltage(T_j =300K/400K)	$V_{th}\ (V)$	4.3 / 3.5	2.1 / 1.7	1.4 / 1.1	1.1 / 0.9	0.9 / 0.7	*k*
Self-clamping Voltage	$V_{scl}\ (V)$	18	15	7	5	4	-
Electron injection efficiency($J=200A/cm^2$)	γ_E	72%	72%	72%	72%	72%	*1*

Scaling rule: *Parameters of scaled (k=2,3,4,5) devices = Parameters of conventional (k=1) device ÷ Scaling factor*

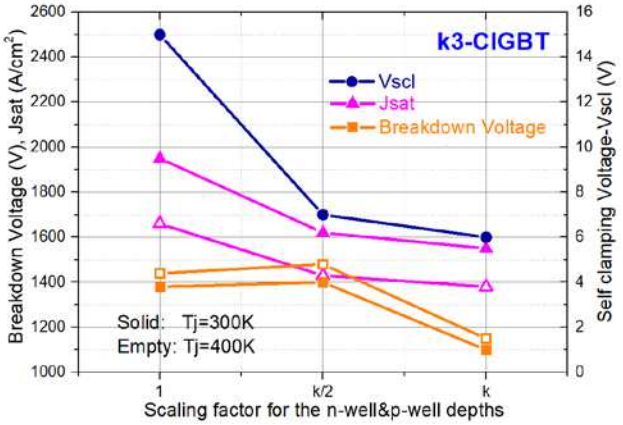

Fig. 5. Influence of n-well/p-well depths scaling factors upon the breakdown voltages, saturation current densities and self-clamping voltages of k3-CIGBT.

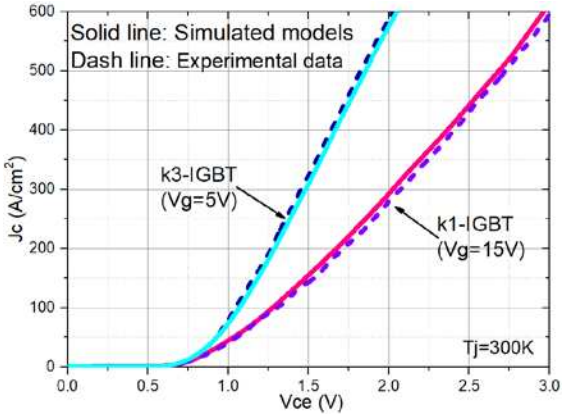

Fig. 6. Comparison of IV characteristics between calibrated models and experimental data in [3]. The models are then used in the analysis of TCIGBT.

should be noted that additional scaling rule for the n-well and p-well depths are carefully selected as a factor of *k/2*. This is because the scaling rule on the n-well and p-well regions is determined by the blocking capability as well as current saturation characteristics. Fig. 5 shows the influence of the n-well/p-well depths scaling factors upon breakdown voltages, saturation current densities and self-clamping voltages of the k3-CIGBT. As the p-well/n-drift junction is the main junction to support blocking voltage, the thickness of the scaled p-well must be sufficient to avoid punch-through before avalanche breakdown. If the p-well depth is scaled with *k*, the p-well region is completely depleted before the electric field reaches its critical value under blocking state. This causes cathode cells to be exposed to high voltages and induces premature breakdown. Saturation current density can be reduced by lowering the punch-through voltage and reducing the n-well depth is a direct solution to achieve this. However, the reduction of n-well depth is limited by the turn-on mechanism of TCIGBT. During turn-on process, the n-well layer must provide a sufficient barrier to prevent holes from flowing into the cathode before the thyristor is triggered. Otherwise, the I-V characteristics will display a snap-back. Consequently, the scaling factor for the n-well/p-well depths are chosen as *k/2*. This will ensure that the scaled devices meet the required blocking capability as well as enable large SOA.

III. SIMULATION RESULTS AND ANALYSIS

The electrical characteristics of the scaled devices are demonstrated by using the 3-dimensional TCAD tools within Synopsys Sentaurus Device [14]. A minority carrier ambipolar lifetime of 10 µs is considered as default. In addition, the IGBT models used in this work are calibrated with the experimental results in [4], as shown in Fig. 6. In a 3-dimensional TCIGBT, as shown in Fig. 3(b), due to existence of the n-well and p-well

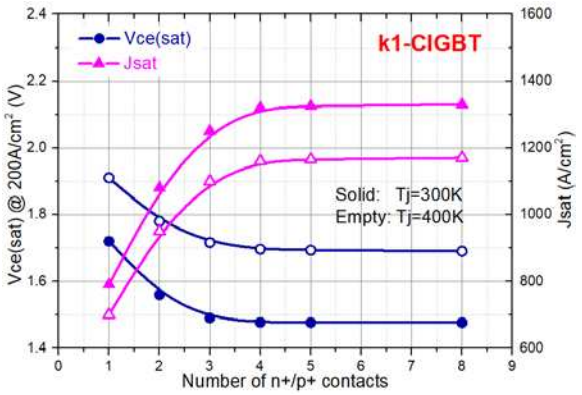

Fig. 7. Influence of $V_{ce(sat)}$ and Jsat on number of n^+/p^+ contacts of k1-TCIGBT.

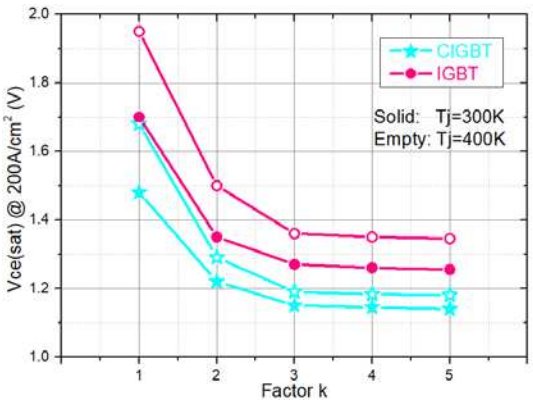

Fig. 9. Vce(sat) dependence on scaling factor k.

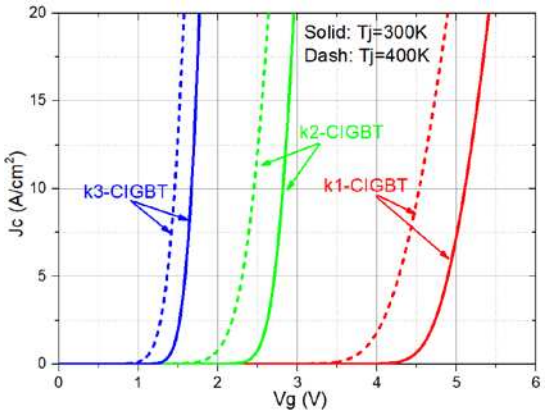

Fig. 8. Input characteristics of the conventional and scaled devices.

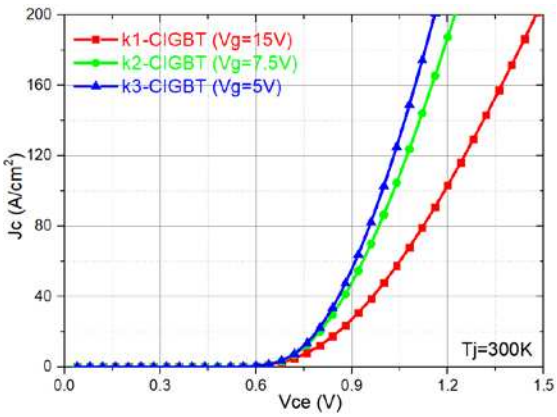

Fig. 10. I-V characteristics of the conventional and scaled devices.

margins, the number of n^+/p^+ contacts employed within a cluster cell influences the electrical characteristics. For the conventional device (k=1), the variations in forward voltage drops and saturation current densities as a function of number of n^+/p^+ contacts are shown in Fig. 7. It shows that the $V_{ce(sat)}$ reduces with increasing number of n^+/p^+ contacts while the J_{sat} increases with increased number of contacts. However, both $V_{ce(sat)}$ and J_{sat} saturate when contact number exceeds four. Therefore, the simulated k1-TCIGBT involves four n^+/p^+ contacts to provide a more accurate simulation results. Similarly, for an identical device area the k3-TCIGBT employs twelve n^+/p^+ contacts.

A. Input Characteristics

To reduce the gate voltage with scaling factor k, the threshold voltage V_{th} should also be adjusted by changing p-base doping. As shown in TABLE I, the scaling rule for the threshold voltages is also available when the junction temperature is increased to 400 K. Hence, the various gate voltages enable the scaled TCIGBT devices tend to be suitable for different digital integrated circuits. Fig. 8 shows the input characteristics of the conventional and scaled devices. The transconductance of the scaled devices are improved compared to the conventional device as a result of reduced channel length as well as scaled gate oxide thickness. Moreover, the reduction of gate oxide thickness is beneficial to improve the I-V characteristics because of the significantly reduced channel resistance R_{ch}, as expressed in (1), where L_{ch} is the vertical channel length, Z is the sum of n+ length, μ_{ni} is the inversion layer mobility, and C_{ox} is the gate oxide capacitance.

$$R_{ch}{}' = \frac{L_{ch}/k}{Z \cdot \mu_{ni} \cdot (k \cdot C_{ox}) \cdot [(V_g - V_{th})/k]} = R_{ch}/k \qquad (1)$$

B. I-V Characteristics

Fig. 9 shows the comparison of on-state voltage drops as a function of k between TCIGBTs and benchmark TIGBTs. In both TIGBT and TCIGBT devices, significant decrease in on-state voltage drop are observed because of scaling rules and tend to saturate when k exceeds 3. However, in conventional and scaled cases, the TCIGBTs show approximately 15% reduction in the on-state voltage drops when compared to the equivalent TIGBTs at Tj=300 K and Tj=400 K. This is because the thyristor effect offers enhanced conductivity modulation in the TCIGBT. Furthermore, the forward voltage drops of the TCIGBTs are less sensitive to the increase in temperature compared to that of the TIGBTs. Fig. 10 shows the linear I-V characteristics of conventional and scaled TCIGBTs. The linear I-V characteristics of the k3-TCIGBT is significantly improved because of the enhancement of thyristor action, which is discussed further in next paragraph. Therefore, the k3-TCIGBT can achieve a very low $V_{ce(sat)}$ of 1.15 V and 1.19 V at Tj=300 K and Tj=400 K, respectively at a current density of 200 A/cm^2.

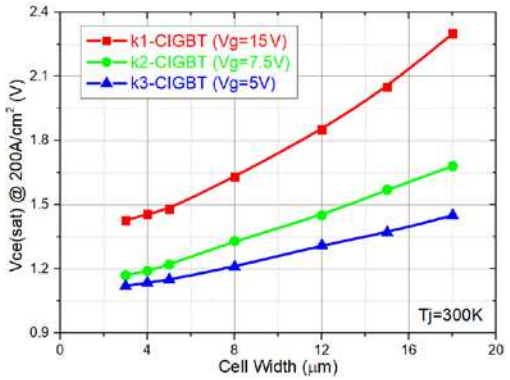

Fig. 11. Vce(sat) dependence on cell width.

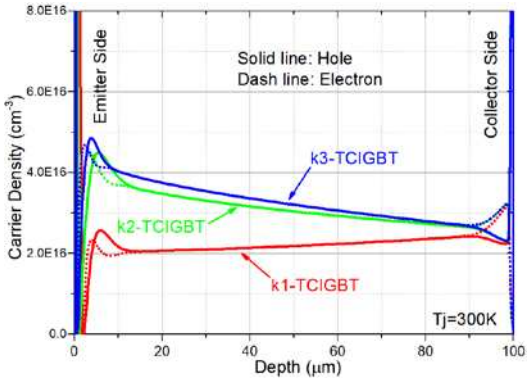

Fig. 12. Carrier distributions within k1-TCIGBT structure and scaled structures at J = 200 A/cm^2.

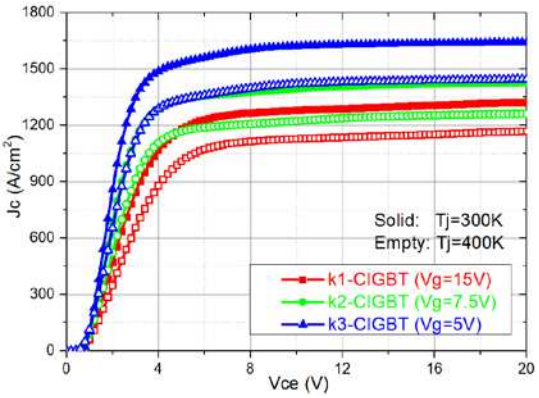

Fig. 13. Current saturation characteristics of the conventional and scaled devices.

It should also be noted that, as shown in TABLE I, the electron injection efficiency does not change with scaling of the device. Hence, IE effect is not presented in the TCIGBT structure. This is further substantiated from Fig. 11 because the $V_{ce(sat)}$ of conventional and scaled devices increase linearly with increase in cell widths. In fact, the improvement of on-state performance is mainly contributed by enhancement of thyristor effect.

Fig. 12 shows the on-state carrier distributions by comparing the scaled TCIGBT devices to the conventional TCIGBT (k=1). A much higher carrier concentration is seen in k3 because of the enhanced thyristor action. The junction injection efficiency of the n-well/p-well junction can be expressed as in (2), where D_p

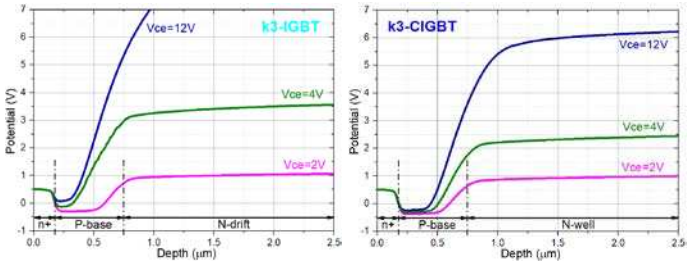

(a) (b)

Fig. 14. Comparison of potential distributions within the middle of mesa regions between (a) k3-IGBT and (b) k3-CIGBT. (Tj = 300 K)

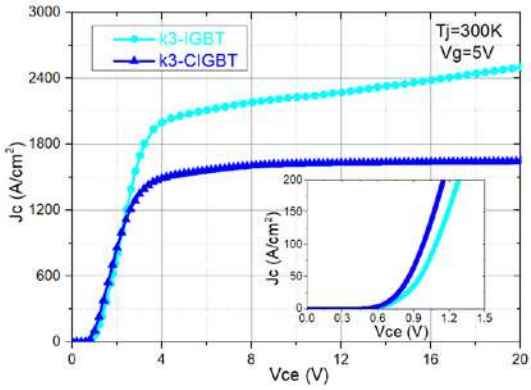

Fig. 15. Comparison of I-V characteristics between k3-IGBT and k3-CIGBT.

and D_n are the minority carrier diffusion coefficient, which are constant, while Q_p and Q_n are the effective charge of the p-well and n-well regions, respectively. For the k3-TCIGBT, the significant decrease of the Q_p/Q_n ratio results in a higher γ [see (3) and (4)]. Hence, the current gain of the n-well/p-well/n-drift transistor β is increased due to higher emitter injection efficiency [see (5) and (6)]. In the k3-TCIGBT structure, the thyristor effect is significantly enhanced, due to increased current gain as well as reduction in MOS channel resistance, which results in the improvement of its on-state performance.

$$\gamma \cong \frac{1}{1+\frac{D_p Q_p}{D_n Q_n}} \tag{2}$$

$$k1: \frac{Q_p}{Q_n} = 1.51 > \; k3: \frac{Q_p}{Q_n} = 0.56 \tag{3}$$

$$\gamma_{k1} < \gamma_{k3} \tag{4}$$

$$\beta = \frac{\gamma}{1-\gamma} = \frac{1}{(1/\gamma)-1} \tag{5}$$

$$\beta_{k1} < \beta_{k3} \tag{6}$$

C. Current Saturation Characteristics

Fig. 13 shows the current saturation characteristics of the conventional TCIGBT and scaled devices. The self-clamping feature in the TCIGBT technology ensures that current saturation levels do not increase significantly as *k* increases. In contrast, the scaling work on IGBT technology suffers from the

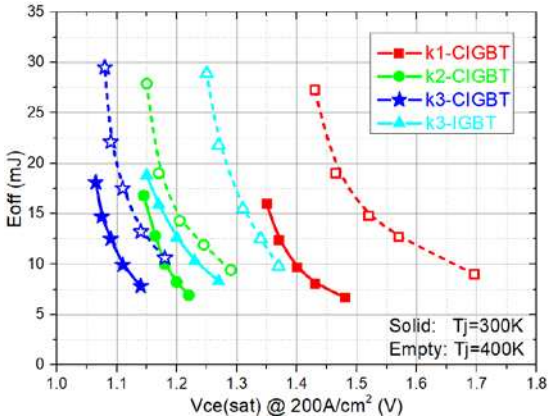

Fig. 16. Comparison of Vce(sat)-Eoff trade-offs at J = 200 A/cm^2. Each line is a variation of P-anode doping concentration from 5e17 cm^{-3} to 1e19 cm^{-3}

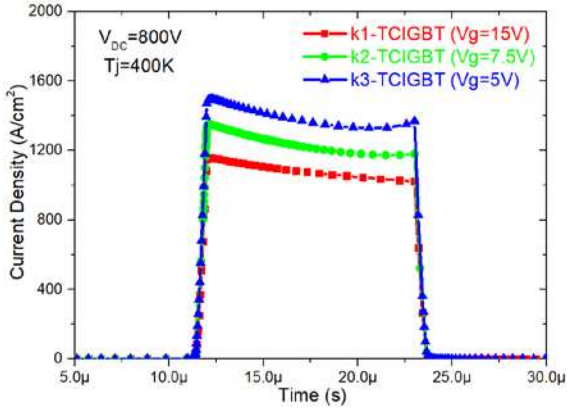

Fig. 17 Short circuit characteristics of conventional and scaled devices.

absence of current saturation, which is originated by the potential barrier lowering in the middle of mesa regions [8]. Fig. 14 depicts the on-state potential distributions within the mesa regions of the k3-TCIGBT device compared to a k3-IGBT device. As shown, the potential barrier of the n+/p-base junction in an IGBT reduces significantly with increased collector voltage. Under this condition, the bipolar carriers flow is enhanced and the current does not show clear saturation, as shown in Fig. 15. This will finally degrade the short circuit robustness and reduce the SOA of an IGBT. This problem can be effectively suppressed with TCIGBT technology due to the self-clamping feature. The potential in the n-well region is clamped and the potential barrier of the n+/p-base junction shows no obvious increase and tends to be independent of collector voltages. This is one major attractive feature over the TIGBT. It should also be noted from Fig. 15 that despite the k3-CIGBT shows lower $V_{ce(sat)}$ in the linear I-V characteristics, 1/3 reduction in saturation current density can be achieved compared to that of the k3-IGBT.

D. Dynamic Characteristics

The dynamic characteristics of the conventional and scaled devices are investigated by using inductive switching simulations. In the inductive switching test circuit, the DC bias is 600 V, the rated current is 100 A (at J=200 A/cm^2) and the stray inductance is 100 nH. Fig. 16 shows the $V_{ce(sat)}$-E_{off} trade-off relationships of comparing the scaled devices to the conventional device as well as benchmark k3-TIGBT, from which much-improved trade-off in comparison to conventional device (k=1) is clear. For an identical E_{off}, k3-TCIGBT can reduce the $V_{ce(sat)}$ by 20% and 30% at Tj = 300K and Tj = 400K, respectively. Moreover, k3-TCIGBT even displays a 10% reduction in $V_{ce(sat)}$ compared to the calibrated k3-IGBT device at Tj = 300K and Tj = 400K.

E. Short-Circuit Performance

The short-circuit withstand time prior to failure is directly related to the saturation current level. The device is expected to withstand short-circuit condition for at least 10 µs. Fig. 17 shows the simulated short-circuit collector current waveforms. The initial junction temperature is set as 400 K while the thermal resistance from the collector electrode to ambient is set as 0.8 cm^2 K/W. It clearly shows that the scaled devices can achieve more than 10 µs short-circuit performance. This short circuit robustness is contributed by self-clamping feature which helps to maintain the saturation current levels.

IV. CONCLUSION

In conclusion, a 3-dimensional scaling rule for 1.2-kV TCIGBT technology is proposed and demonstrated. The calibrated 3-dimensional simulation results show that the 3-dimensional scaling can realize much improved $V_{ce(sat)}$-E_{off} trade-offs in a TCIGBT while maintaining short-circuit withstand capability. Due to the enhancement of thyristor effect, the on-state voltage drop can be reduced significantly without degrading short-circuit withstand capability. The unique self-clamping feature successfully controls the saturation current levels and therefore enable the scaled devices to remain short circuit robustness, which tends to break the application limit of scaling rule in trench IGBTs.

REFERENCES

[1] A. Mittal, "Energy efficiency enabled by power electronics," in *2010 International Electron Devices Meeting*, 2010, pp. 1.2.1-1.2.7.
[2] "More-than-Moore",White paper, ITRS; 2010.
[3] M. Tanaka and I. Omura, "Scaling rule for very shallow trench IGBT toward CMOS process compatibility," in *2012 24th International Symposium on Power Semiconductor Devices and ICs*, 2012, pp. 177-180.
[4] K. Kakushima, T. Hoshii, K. Tsutsui, A. Nakajima, S. Nishizawa, H. Wakabayashi, *et al.*, "Experimental verification of a 3D scaling principle for low Vce(sat) IGBT," in *2016 IEEE International Electron Devices Meeting (IEDM)*, 2016, pp. 10.6.1-10.6.4.
[5] M. Kitagawa, I. Omura, S. Hasegawa, T. Inoue, and A. Nakagawa, "A 4500 V injection enhanced insulated gate bipolar transistor (IEGT) operating in a mode similar to a thyristor," in *Proceedings of IEEE International Electron Devices Meeting*, 1993, pp. 679-682.
[6] H. Feng, W. Yang, Y. Onozawa, T. Yoshimura, A. Tamenori, and J. K. O. Sin, "A 1200 V-class Fin P-body IGBT with ultra-narrow-mesas for low conduction loss," in *2016 28th International Symposium on Power Semiconductor Devices and ICs (ISPSD)*, 2016, pp. 203-206.
[7] C. Jaeger, A. Philippou, A. V. Ilei, J. G. Laven, and A. Härtl, "A new sub-micron trench cell concept in ultrathin wafer technology for next generation 1200 V IGBTs," in *2017 29th International Symposium on Power Semiconductor Devices and IC's (ISPSD)*, 2017, pp. 69-72.
[8] K. Eikyu, A. Sakai, H. Matsuura, Y. Nakazawa, Y. Akiyama, Y. Yamaguchi, *et al.*, "On the scaling limit of the Si-IGBTs with very narrow mesa structure," in *2016 28th International Symposium on Power Semiconductor Devices and ICs (ISPSD)*, 2016, pp. 211-214.

[9] M. Tanaka and A. Nakagawa, "Conductivity modulation in the channel inversion layer of very narrow mesa IGBT," in *2017 29th International Symposium on Power Semiconductor Devices and IC's (ISPSD)*, 2017, pp. 61-64.
[10] O. Spulber, M. Sweet, K. Vershinin, C. K. Ngw, L. Ngwendson, J. V. S. C. Bose, *et al.*, "A novel trench clustered insulated gate bipolar transistor (TCIGBT)," *IEEE Electron Device Letters*, vol. 21, pp. 613-615, 2000.
[11] D. Kumar, M. Sweet, K. Vershinin, L. Ngwendson, and E. M. S. Narayanan, "RC-TCIGBT: A Reverse Conducting Trench Clustered," in *Proceedings of the 19th International Symposium on Power Semiconductor Devices and IC's*, 2007, pp. 161-164.
[12] N. Luther-King, M. Sweet, and E. M. S. Narayanan, "Clustered Insulated Gate Bipolar Transistor in the Super Junction Concept: The SJ-TCIGBT," *IEEE Transactions on Power Electronics*, vol. 27, pp. 3072-3080, 2012.
[13] K. Vershinin, M. Sweet, L. Ngwendson, J. Thomson, P. Waind, J. Bruce, *et al.*, "Experimental Demonstration of a 1.2kV Trench Clustered Insulated Gate Bipolar Transistor in Non Punch Through Technology," in *2006 IEEE International Symposium on Power Semiconductor Devices and IC's*, 2006, pp. 1-4.
[14] I. Synopsys, *Sentaurus Device User Guide*: Ver. L-2016.03.

Peng Luo received the M.S. degree from the University of Sheffield, Sheffield, U.K., in 2015, where he is currently working toward the Ph.D. degree in the Electrical Machines and Drives Group, Department of Electronic and Electrical Engineering.

His research is focused upon the development and implementation of power semiconductor devices.

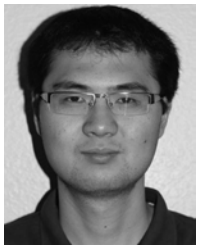

Hong Yao Long was born in Taiyuan, China. He received the B.Eng. (Hons.) and Ph.D. degrees from the University of Sheffield, Sheffield, U.K., in 2007 and 2012, respectively.

His research interests include device modeling, gate drive control system for MOS-gate power devices, and reliability issues.

Mark R. Sweet received the B.Sc. (Hons.) degree in electronics engineering and the Ph.D. degree in high voltage micro-electronics from De Montfort University, Leicester, U.K., in 1998 and 2004, respectively.

In 2007, he joined the University of Sheffield, Sheffield, U.K., as a Research Fellow, and involved in the field of converter power density.

Maria Merlyne De Souza received the B.Sc. from the University of Bombay, Mumbai, India, in 1985; the B.E. degree from the Indian Institute of Science, Bangalore, India, in 1988; and the Ph.D. degree from the University of Cambridge, Cambridge, U.K., in 1994.

She is currently a Professor with the Deparment of Electronic and Electrical Engineering, The University of Sheffield, Sheffield, U.K.

Ekkanath Madathil Sankara Narayanan received the B.Sc. and M.Sc. degrees from the PSG College of Technology, Coimbatore, India, the M.Tech. degree from the Indian Institute of Science, Bangalore, India, and the Ph.D. degree from the University of Cambridge, Cambridge, U.K.

He is currently a Professor with the Deparment of Electronic and Electrical Engineering, The University of Sheffield, Sheffield, U.K.